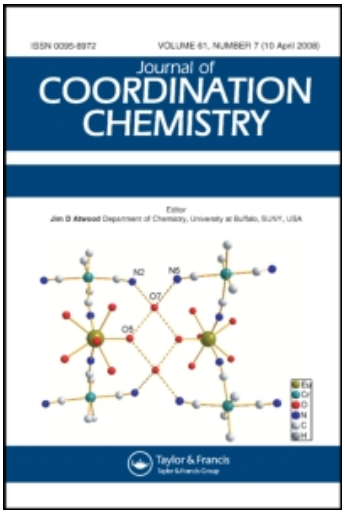

Journal of Coordination Chemistry
Publication details, including instructions for authors and subscription information:
http://www.informaworld.com/smpp/title~content=t713455674

Synthesis, molecular, crystal and electronic structure of $[(C_6H_6)Ru(1,2,4\text{-triazole})_3](CF_3SO_3)_2$

J. G. Małecki[a]; R. Kruszynski[b]; M. Jaworska[c]; P. Lodowski[c]
[a] Department of Inorganic and Radiation Chemistry, Institute of Chemistry, University of Silesia, Katowice 40-006, Poland [b] Department of X-ray Crystallography and Crystal Chemistry, Institute of General and Ecological Chemistry, Łódź University of Technology, Poland [c] Department of Theoretical Chemistry, Institute of Chemistry, University of Silesia, Katowice 40-006, Poland

To cite this Article Małecki, J. G. , Kruszynski, R. , Jaworska, M. and Lodowski, P.(2007) 'Synthesis, molecular, crystal and electronic structure of $[(C_6H_6)Ru(1,2,4\text{-triazole})_3](CF_3SO_3)_2$', Journal of Coordination Chemistry, 60: 7, 741 — 751
To link to this Article: DOI: 10.1080/00958970600914796
URL: http://dx.doi.org/10.1080/00958970600914796

Journal of Coordination Chemistry
Vol. 60, No. 7, 10 May 2007, 741–751

Taylor & Francis
Taylor & Francis Group

Synthesis, molecular, crystal and electronic structure of $[(C_6H_6)Ru(1,2,4\text{-triazole})_3](CF_3SO_3)_2$

J. G. MAŁECKI*†, R. KRUSZYNSKI‡, M. JAWORSKA§ and P. LODOWSKI§

†Department of Inorganic and Radiation Chemistry, Institute of Chemistry, University of Silesia, 9th Szkolna Street, Katowice 40-006, Poland
‡Department of X-ray Crystallography and Crystal Chemistry, Institute of General and Ecological Chemistry, Łódź University of Technology, 116 Żeromski Street, Łódź 90-924, Poland
§Department of Theoretical Chemistry, Institute of Chemistry, University of Silesia, 9th Szkolna Street, Katowice 40-006, Poland

(*Received in final form 21 April 2006*)

$[(C_6H_6)Ru(1,2,4\text{-triazole})_3](CF_3SO_3)_2$ has been prepared and studied by IR, electronic and ^1H NMR spectroscopy and X-ray crystallography. The complex was prepared by reaction of $[(C_6H_6)RuCl_2]_2$ with 1,2,4-triazole in the presence of $AgCF_3SO_3$ in methanol. The electronic spectrum of the compound has been calculated using the TDDFT method.

Keywords: Ruthenium; Arene; 1,2,4-Triazole; X-ray structure; Bond valence; DFT; TDFFT; CASPT2

1. Introduction

η^6-Arene ruthenium complexes play a vital role in organometallic chemistry [1a–e]. The arene ruthenium halide compounds, obtained by Winkhaus and Singer [2], are key starting materials for the formation of a wide range of neutral and cationic ligand derivatives [1d, 3a–d]. Half-sandwich arene ruthenium complexes may serve as excellent catalyst precursors for hydrogenation [3c, 4a–e] and for ring-opening metathesis polymerization [4f]. Recent studies of arene ruthenium complexes have shown that they are found to inhibit cancer cell growth [5a–d]. 1,2,4-Triazole is of considerable interest as a ligand because of its presence in many biological systems (fungicides, herbicides, pharmaceutics) [6a–c]. Activity is enhanced if triazole exists as a metallic complex [7a–c].

In the last decade, density functional theory (DFT) has become a very popular computational method for the calculation of a number of molecular properties [8a–e]. Because of its greater computational efficiency, DFT has been applied extensively to

*Corresponding author. Email: gmalecki@us.edu.pl

Journal of Coordination Chemistry
ISSN 0095-8972 print/ISSN 1029-0389 online © 2007 Taylor & Francis
DOI: 10.1080/00958970600914796

inorganic and organometallic complexes [9a–e]. The time-dependent generalization of DFT (TDDFT) offered a rigorous route to calculate the dynamic response of charge density [10a–c]. The reliability of the TDDFT approach in obtaining accurate predictions of excitation energies and oscillator strengths is well documented. The method has been successfully used to calculate the electronic spectra of transition metal complexes with a variety of ligands [11a–f]. It was found that the TDDFT method gives fairly accurate results for valence excited states but incorrectly describes long-range excited states of CT character. This failure was ascribed to the self-interaction error in DFT or alternatively to incorrect asymptotic behaviour of the approximate density functional [12]. The influence of the contribution of the HF exchange in hybrid functionality on the calculated energies of CT states was studied for ruthenium complexes [12d]. In this article, we present the synthesis, crystal structure, spectroscopic properties and the electronic structure of the first benzene ruthenium(II) complex with 1,2,4-triazole ligands.

2. Experimental

The starting material $[(C_6H_6)RuCl_2]_2$ was synthesized according to a literature procedure [13]. All other reagents were commercially available and used without further purification.

2.1. *[(C$_6$H$_6$)Ru(triazol)$_3$](CF$_3$SO$_3$)$_2$*

A suspension of $[(C_6H_6)RuCl_2]_2$ (0.25 g, 5×10^{-4} mol) and $AgCF_3SO_3$ (1.0 g) in methanol (80 cm^3) was stirred in the dark for 2 h. Precipitated AgCl was filtered off and to the yellow solution 1,2,4-triazole (0.5 g) in 20 cm^3 of methanol was added. The mixture was stirred for 3 h. Crystals suitable for X-ray analysis were obtained by slow evaporation of the solution. Yield: 41%. IR (KBr): 3126 ν_{NH}; 3002, 2906, 2832 ν_{CH}; 1530 ν_{CN}; 1422 $\nu_{C=C}$; 1294 $\delta_{(triazole)}$; 1039 $\delta_{(N–N,\ N–C\ in\ the\ plane)}$; 834 $\delta_{(C–C\ benzene)}$; 633 $\delta_{(N–N,\ N–C\ out\ of\ plane)}$. ^{1}H NMR ($\delta$, acetone-d$_6$): 14.2 (s, 1H), 8.98 (s, 2H), 6.28 (s, 6H). Electronic spectrum (nm, CH_2Cl_2) (log ε): 546.6 (1.23), 365.2 (1.74), 280 (sh), 260 (sh), 230 (sh), 212.2 (2.98). Anal. Calcd for $C_{14}H_{15}F_6N_9O_6RuS_2$ (%): C, 24.57; H, 2.21; N, 18.42; O, 14.02. Found: C, 24.59; H, 2.20; N, 18.39; O, 13.97.

2.2. *Physical measurements*

IR spectra (KBr pellets) were recorded on a Nicolet Magna 560 spectrophotometer in the range 4000–400 cm^{-1}. Electronic spectra were measured on a Lab Alliance UV-VIS 8500 spectrophotometer in the range 800–280 nm in deoxygenated dichloromethane solution. Elemental analyses (C, H, N) were performed on a Perkin-Elmer CHN-2400 analyser. The ^{1}H NMR spectrum was obtained at room temperature in acetone-d$_6$ using an INOVA 300 spectrometer.

2.3. *Computational details*

The Gaussian-03 program [14] was used in the calculations. Geometry optimization was carried out with the DFT method with the use of B3LYP functions [15, 16]. Electronic transitions were calculated with the PCM model [17] with methanol solution as solvent. The calculation was performed using the DZVP basis set [18] with f functions with exponents 1.94722036 and 0.748930908 on the ruthenium atom, and polarization functions for all other atoms: 6-31g(2d,p) chlorine, 6-31g** carbon, nitrogen, 6-31g(d,p) hydrogen.

CASPT2 [19] calculations were performed with the use of the MOLCAS-5 program [20]. The LANL2DZ with ECP for ruthenium was used. The ANO-L basis [21] (14s9p4d/3s2p1d) was used for carbon and nitrogen and ANO-L (8s/2s) for hydrogen.

2.4. *Crystal structure determination*

A yellow plate of $[(C_6H_6)Ru(1,2,4\text{-}C_2H_3N_3)_3](CF_3SO_3)_2$ was mounted on a KM-4-CCD automatic diffractometer equipped with a CCD detector, and used for data collection. X-ray intensity data were collected with graphite-monochromated Mo-Kα radiation ($\lambda = 0.71073$ Å) at 293.0(2) K, with the ω scan mode. A 55 second exposure time was used and all Ewald sphere reflections were collected up to $2\theta = 50.20^\circ$. Unit cell parameters were determined from least-squares refinement of the setting angles of the 2218 strongest reflections. Details concerning crystal data and refinement are given in table 1. Examination of two reference frames monitored after each 20 frames measured

Table 1. Crystal data and structure refinement details for $[(C_6H_6)Ru(C_2H_3N_3)_3](CF_3SO_3)_2$.

Empirical formula	$C_{14}H_{15}F_6N_9O_6RuS_2$
Formula weight	684.54
Temperature (K)	293(2)
Crystal system	Monoclinic
Space group	*Cm*
Unit cell dimensions (Å, °)	
a	8.6409(12)
b	19.271(2)
c	7.0020(9)
β	96.337(11)
Volume (Å^3)	1158.8(3)
Z	2
Calculated density (Mg m^{-3})	1.962
Absorption coefficient (mm^{-1})	0.959
F(000)	680
Crystal dimensions (mm^3)	$0.537 \times 0.102 \times 0.016$
θ range for data collection (°)	2.93–25.10
Index ranges	$-10 \le h \le 8$, $-22 \le k \le 22$, $-8 \le l \le 8$
Reflections collected	6066
Independent reflections	1920 [$R_{(int)} = 0.1222$]
Data/restraints/parameters	1920/2/186
Goodness-of-fit on F^2	0.983
Final *R* indices [$I > 2\sigma(I)$]	$R_1 = 0.0550$, $wR_2 = 0.1073$
R indices (all data)	$R_1 = 0.0636$, $wR_2 = 0.1110$
Largest diff. peak and hole (e Å^{-3})	0.935 and −0.499

showed 9.73% loss of the intensity. During the data reduction, the above decay correction coefficient was taken into account. Lorentz, polarization, and numerical absorption [22] corrections were applied. The structure was solved by direct methods. All non-hydrogen atoms were refined anisotropically using full-matrix, least-squares techniques on F^2. All hydrogen atoms were found from difference Fourier syntheses after four cycles of anisotropic refinement, and refined as riding on the adjacent atom with an individual isotropic temperature factor equal to 1.2 times the value of equivalent temperature factor of the parent atom. SHELXS97 [23], SHELXL97 [24] and SHELXTL [25] programs were used for all calculations. Atomic scattering factors were those incorporated in the computer programs.

3. Results and discussion

3.1. *Crystal structure*

The half-sandwich $[(C_6H_6)Ru(1,2,4\text{-}C_2H_3N_3)_3](CF_3SO_3)_2$ complex was obtained by the reaction of $[(C_6H_6)RuCl_2]_2$ with 1,2,4-triazole in presence of Ag CF_3SO_3 in methanol. The elemental analysis of the complex is in good agreement with the formulation. Characteristic bands of the triazole ligands ν(CN) at 1530 cm^{-1} and ν(C=C) at 1422 cm^{-1} are present in the IR spectrum of the complex. In the ^{1}H NMR spectrum of the complex the protons of the C_6H_6 ligand appears as a singlet at 6.28 ppm. The 1,2,4-triazole protons resonate at 14.2 ppm (NH) and 8.98 (CH).

$[(C_6H_6)Ru(1,2,4\text{-}C_2H_3N_3)_3](CF_3SO_3)_2$ crystallises in the monoclinic space group *Cm*. The Ru(1) atom, two atoms of the benzene ring (C(5) and C(8)) and the triazole ring indicated by the N(1) atom lie on a mirror (special positions *a* of space group *Cm* at *x*, 0, *y* [26]) and all other atoms lie in general positions. The molecular structure of the compound (two asymmetric units) is shown in figure 1. Selected bond lengths and angles are listed in table 2.

The ruthenium atom is in a formally six-coordinate environment, and the structure of the cation $[(C_6H_6)Ru(1,2,4\text{-}C_2H_3N_3)_3]^+$ adopts a distorted piano-stool geometry with angles around ruthenium of 87.6(3)° (N(1)–Ru–N(4)), 86.6(4)° (N(4)–Ru–N(4A)), 87.2(4)° (N(4A)–Ru(1)–C(6)). The ruthenium atom is π-bonded to the benzene ring with an average Ru–C distance of 2.159(14) Å (range 2.145(14)–2.170(2) Å). The distance between the ruthenium atom and the centroid of the benzene ring is 1.674 Å and is consistent with those reported for the other Ru(II) η^6-arene complexes [3d, 27, 28]. The ruthenium atom is also coordinated to nitrogen atoms of 1,2,4-triazole ligands with distances 2.109(12) and 2.117(8) Å.

Bond valences were computed as $v_{ij} = \exp[(R_{ij} - d_{ij})/b]$ [29–31], where R_{ij} is the bond-valence parameter (in the formal sense the R_{ij} parameter value can be considered as an idealised single-bond length between *i* and *j* atoms). R_{Ru-N} and $R_{Ru-\pi}$ were taken as being 1.656, 1.731 [32], respectively, and *b* was taken as 0.37 [29]. Computed bond valences of ruthenium are $v_{Ru-N} = 0.294$, 0.288 and $v_{Ru-\pi} = 0.944$ v.u. (valence units) which means that Ru–π bond is almost four times stronger than other bonds. The valence sum rule states that the sum of the valences of the bonds formed by an atom is equal to the valence of the atom, and only the difference larger than 0.23–0.30 can be a

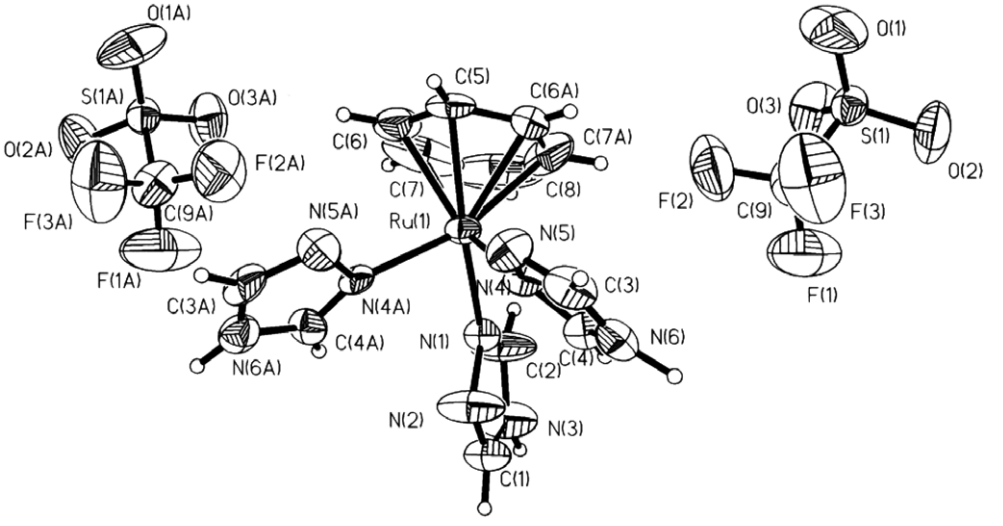

Figure 1. ORTEP drawing of $[(C_6H_6)Ru(C_2H_3N_3)_3](CF_3SO_3)_2$ with 50% probability displacement ellipsoids, showing the atom labelling scheme.

Table 2. Selected bond lengths (Å) and angles (°) for $[(C_6H_6)Ru(C_2H_3N_3)_3](CF_3SO_3)_2$.

Experimental		Optimised	Experimental		Optimised
Ru(1)–N(1)	2.109(12)	2.16	N(1)–Ru(1)–N(4)	87.6(3)	89.90
Ru(1)–N(4)	2.117(8)	2.20	N(1)–Ru(1)–C(7)	104.3(6)	104.56
Ru(1)–C(6)	2.157(9)	2.26	N(4)–Ru(1)–C(7)	164.8(4)	163.46
Ru(1)–C(7)	2.145(14)	2.26	N(1)–Ru(1)–C(6)	136.7(4)	137.23
Ru(1)–C(5)	2.164(14)	2.29	N(4)–Ru(1)–C(6)	134.9(4)	131.93
Ru(1)–C(8)	2.170(2)	2.29	N(1)–Ru(1)–N(4A)	87.6(3)	84.05
S(1)–O(3)	1.398(7)		N(4A)–Ru(1)–C(7)	103.1(6)	103.64
S(1)–O(1)	1.418(9)		N(4A)–Ru(1)–C(6)	87.2(4)	86.75
S(1)–O(2)	1.421(7)		C(6)–Ru(1)–C(6A)	66.8(6)	65.56
S(1)–C(9)	1.829(15)		N(4)–Ru(1)–N(4A)	86.6(4)	84.05
C(9)–F(1)	1.247(14)		N(4)–Ru(1)–C(6A)	87.2(4)	86.75
C(9)–F(3)	1.262(16)		N(1)–Ru(1)–C(7A)	104.3(6)	103.64
C(9)–F(2)	1.314(15)		C(6)–Ru(1)–C(8)	66.8(6)	65.70
			C(7A)–Ru(1)–C(6)	77.7(5)	76.96
			N(1)–Ru(1)–C(5)	167.8(4)	168.11

reasonable guide to those structural studies that should be examined in more detail because of possible errors [33]. The computed total valence of the Ru atom is 1.813 v.u.

Nine intermolecular hydrogen bonds [34–36] linking the trifluoromethanesulphonate anion and the cation and two between triazole N–H and N(N(3)–H(3N)$\cdots$N(5)(#$2x+1, y, z$), N(3)–H(3N)$\cdots$N(5)(#$3x+1, -y, z$) are observed (table 3). In this way a three-dimensional, infinite hydrogen bonded net is created. No significant intermolecular interactions were identified.

Table 3. Hydrogen bonds in $[(C_6H_6)Ru(C_2H_3N_3)_3](CF_3SO_3)_2$ (Å and °).

D–H···A	d(D–H)	d(H···A)	d(D···A)	∠(DHA)
N(3)–H(3N)···N(5)#2	0.99	2.37	3.164(12)	137.0
N(3)–H(3N)···N(5)#3	0.99	2.37	3.164(12)	137.0
N(6)–H(6N)···O(1)#4	1.07	2.52	3.036(12)	108.6
N(6)–H(6N)···O(3)#5	1.07	1.96	2.920(12)	148.2
C(1)–H(1)···O(2)#4	0.93	2.54	3.164(13)	124.9
C(1)–H(1)···O(2)#6	0.93	2.54	3.164(13)	124.9
C(2)–H(2)···O(2)#7	0.93	2.59	3.254(15)	128.8
C(2)–H(2)···O(2)#8	0.93	2.59	3.254(15)	128.8
C(3)–H(3)···O(3)#9	0.93	2.38	3.296(12)	166.7
C(6)–H(6)···F(2)#1	0.93	2.55	3.286(13)	136.6
C(7)–H(7)···O(1)#7	0.93	2.52	3.37(2)	153.0

Symmetry transformations used to generate equivalent atoms, 1: $x, -y, z$; #2: $x+1, y, z$; #3: $x+1, -y, z$; #4: $x+1/2, -y+1/2, z+1$; #5: $x, y, z+1$; #6: $x+1/2, y-1/2, z+1$; #7: $x+1/2, y-1/2, z$; #8: $x+1/2, -y+1/2, z$; #9: $x-1/2, -y+1/2, z+1$.

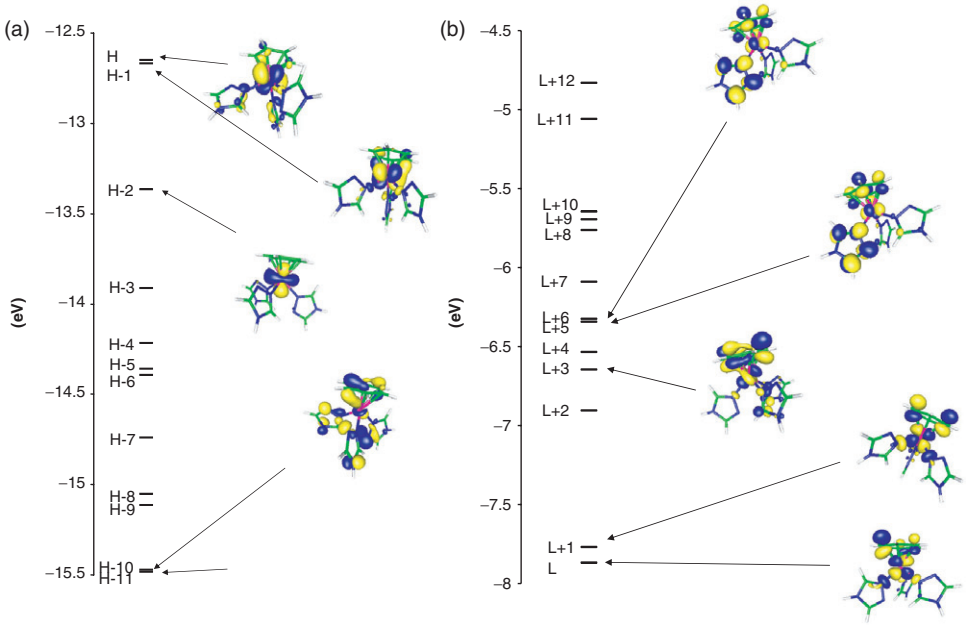

Figure 2. Molecular orbital diagram showing (a) HOMO and (b) LUMO orbitals of $[(C_6H_6)Ru(C_2H_3N_3)_3](CF_3SO_3)_2$.

3.2. *Geometry and electronic structure*

Optimised geometrical parameters for the complex are given in table 2. Optimized bond distances and angles agree with experimental values. The largest differences were found for the ruthenium–benzene carbon distances. The calculated Ru–benzene distance is 1.7508 Å. The formal charge of ruthenium is +2 in the complex. The calculated charge on the ruthenium atom, obtained from natural population analysis is 0.483. The population of the d_{xy}, d_{xz}, d_{yz}, d_{x^2} − d_{y^2} and d_{z^2} orbitals of the central atom is 1.714,

0.864, 1.776, 1.646 and 1.768, respectively. This is a result of charge donation from the benzene ring and triazole ligands. The charge on the benzene ring, obtained from NBO analysis, is close to 0.6026. Charges on 1,2,4-triazole nitrogen donor atoms are negative and amount to −0.307 (N1), −0.549 (N4) and −0.556 (N4A). N1 is less negative, which indicates higher electron density delocalisation towards the ruthenium atom. The HOMO-LUMO gap is 4.65 eV.

The HOMO (62% d_{Ru}), HOMO-1 (63% d_{Ru}), HOMO-2 (87% d_{Ru}) and LUMO (46% d_{Ru}), LUMO+1 (45% d_{Ru}) molecular orbitals are d ruthenium type orbitals with admixture of triazole π orbitals. In figure 2(a) molecular orbital diagram of the complex is presented with several contoured molecular orbitals (HOMO – figure 2a, LUMO – figure 2b). Bonding between benzene and ruthenium involves HOMO-10 and HOMO-11; antibonding is associated with LUMO+1 and LUMO+3. In back-donation (metal to ligand), the occupied ruthenium d orbitals and empty π_4^*, π_5^* benzene orbitals participate (HOMO-1, HOMO and LUMO+5, LUMO+6). Remaining molecular orbitals are composed from AOs of triazole and benzene ligands. HOMO-6, HOMO-8 and HOMO-9 MOs are mainly composed of orbitals of lone pairs localized on uncoordinated nitrogen atoms.

3.3. *Electronic spectrum*

The experimental spectrum of the complex shows bands at 547, 365 and 212 nm with shoulders at about 280, 260 and 230 nm. Electronic transitions of $[(C_6H_6)Ru(1,2,4\text{-}C_2H_3N_3)_3]^{2+}$ were calculated with the TDDFT method using the DZVP basis set on the ruthenium atom. The PCM model with methanol as solvent was used in the calculations. Figure 3 shows experimental (solid line) and calculated (dotted line) spectra. Each calculated transition was represented by a gaussian function with equal oscillator strength and width equal to 0.05. Assignment of the calculated transitions to the experimental bands is based on the energy and oscillator strength of the calculated transitions. In the description of the electronic transitions the main components of the molecular orbital are used. TDDFT-calculated transitions are gathered in table 4.

There is a very low intensity band at 546.6 nm ($\varepsilon = 16$) in the experimental spectrum. In calculated spin-allowed singlet transitions with the TDDFT method there was no transition above 500 nm. Hence, we performed calculations for triplet transitions, and in this region excitations were obtained between 546 and 519 nm. These are of $d \rightarrow d$ (LF) character, and we ascribe them to the band at 546 nm. The experimental band at 365 nm is assigned to calculated singlet transitions between 426 and 363 nm of $d \rightarrow d$ type. They originate from excitations among HOMO, HOMO-1, HOMO-2 and LUMO, LUMO+1 molecular orbitals. The shoulder at 280 nm is assigned to the calculated transition at 244 nm of $d \rightarrow \pi^*_{(benzene)}$ (MLCT) character; the shoulders at 260 and 230 nm are assigned to MLCT transitions ($d \rightarrow \pi^*_{(triazole)}$). The highest energy band at 212 nm is of LMCT and MLCT types involving $n_{(N_{triazole})} \rightarrow d$ and $d \rightarrow \pi^*_{(triazole)}$ transitions.

To verify the TDDFT assignments we performed calculations of electronic transitions with the CASPT2 method. The validity of the assignment of the lowest energy band to the triplet transitions was of special interest. In CASSCF/CASPT2 calculations, the active space of 14 orbitals and 14 electrons was used. C_s symmetry was used in the calculations. The active space consists of the occupied $3d_{x^2-y^2}$ and $3d_{xy}$

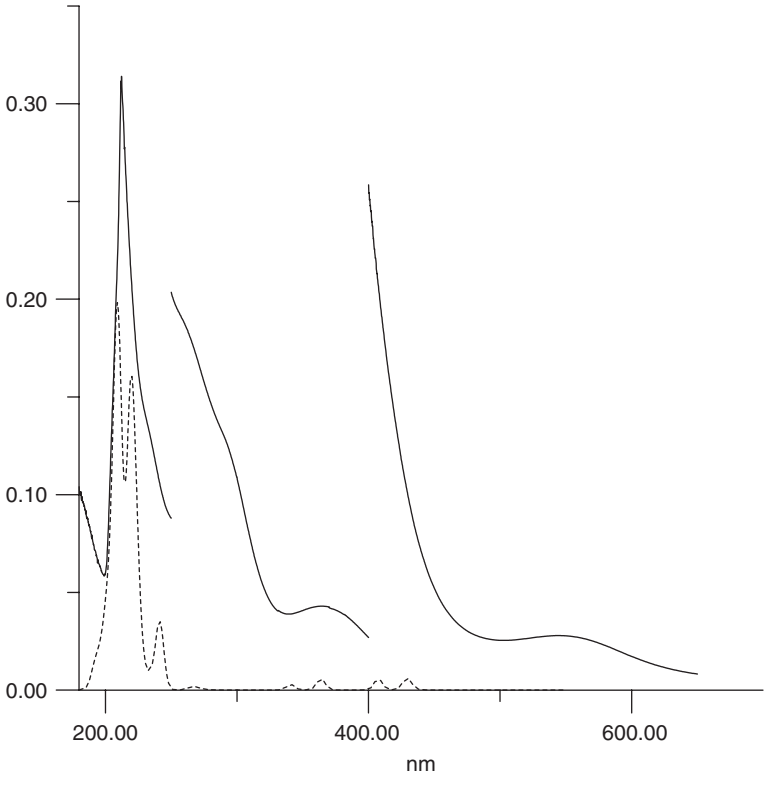

Figure 3. Electronic spectrum of $[(C_6H_6)Ru(C_2H_3N_3)_3](CF_3SO_3)_2$.

orbitals and two correlating π* orbitals of benzene forming two native bonds (metal to ligand donation), the unoccupied $3d_{xz}$ and $3d_{yz}$ orbitals and two correlating benzene π* orbitals (ligand to metal back-donation), the unoccupied $3d_{z^2}$ orbital and a correlating $4d_{z^2}$ orbital, together with two π and two π* orbitals of triazole ligands. Such active space leads to about 1.4 million configurations in the singlet state and 2.5 million in the triplet state. In CASPT2 the level shift parameter 0.3 was used. In the ground state and all excited states the weight of the reference function was similar, about 0.53. In each symmetry 11 singlet electronic transitions were calculated. Several triplet states of both symmetries were also calculated.

In table 5 the CASPT2 calculated singlet transitions with the largest oscillator strength and the triplet transitions are gathered. The calculated CASPT2 transitions correspond to the low energy part of the spectrum. There are no singlet transitions found above 500 nm in the CASPT2 electronic spectrum. The four transitions at 412, 408, 388 and 333 nm of $d \rightarrow d$ character can be assigned to the wide band in the experimental spectrum with a maximum at 365 nm. The weak band at 546 nm is ascribed to the triplet transitions found in CASPT2 between 565 and 503 nm. These transitions are also of $d \rightarrow d$ type. There are calculated singlet transitions at 282 and 279 nm of $d \rightarrow \pi^*_{(benzene)}$ character. These transitions can be ascribed to the shoulder at 280 nm in the experimental spectrum. The transition of similar character is found in the

Table 4. Calculated electronic transitions for $[(C_6H_6)Ru(C_2H_3N_3)_3]^+$ with the TDDFT method.

The most important orbital excitations		Symmetry	λ (nm)	E (eV)	F	Experimental λ(nm) [E(eV)] log ε	Character
			Singlet transitions				
H-1 → L	H → L + 1	A″	426.08	2.909	0.0046	365.2 (3.39)	d → d
H-2 → L		A′	409.99	3.024	0.0048	1.74	d → d
H-2 → L	H-1 → L + 1	A′	363.40	3.412	0.0055		d → d
H-1 → L + 2		A′	244.67	5.067	0.0355	280 (sh)	d → $\pi^*_{(benzene)}$
H-1 → L + 4		A′	232.91	5.323	0.0141	260 (sh)	d → $\pi^*_{(triazole)}$
H-1 → L + 4		A′	222.98	5.560	0.0779		d → $\pi^*_{(triazole)}$
H-1 → L + 5		A′	222.05	5.584	0.0386	230 (sh)	d → $\pi^*_{(triazole)}$
H-1 → L + 5	H → L + 6	A″	215.69	5.748	0.0194		d → $\pi^*_{(triazole)}$
H → L + 7		A′	211.10	5.873	0.0376	212.2 (5.84)	d → $\pi^*_{(triazole)}$
H-8 → L		A′	204.14	6.074	0.0135	2.98	$n_{(Ntriazole)}$ → d
H-8 → L + 1	H→L + 8	A′	200.20	6.193	0.0245		$n_{(Ntriazole)}$ → d d → $\pi^*_{(triazole)}$
H-2 → L + 5		A′	199.93	6.201	0.0373		d → $\pi^*_{(triazole)}$
			Triplet transitions				
		A″	545.90	2.271		546.6 (2.27)	d → d
		A′	544.75	2.276		1.23	d → d
		A′	529.03	2.344			d → d
		A′	519.26	2.388			d → d
		A′	470.57	2.635			d → d
		A′	440.67	2.814			d → d

Table 5. Calculated electronic transitions for $[(C_6H_6)Ru(C_2H_3N_3)_3]^+$ with the CASPT2 method.

Symmetry	(eV)	(nm)	f	Character
Singlet transitions				
A′	3.01	412.00	0.0035	d → d
A″	3.04	408.17	0.0053	d → d
A′	3.19	388.83	0.0032	d → d
A′	3.71	333.98	0.0014	d → d
A″	4.40	282.00	0.0058	d → $\pi^*_{(benzene)}$
A′	4.43	279.73	0.0036	d → $\pi^*_{(benzene)}$
Triplet transitions				
A″	2.19	565.96		d → d
A′	2.33	532.14		d → d
A″	2.44	508.06		d → d
A′	2.46	503.06		d → d
A′	2.72	456.36		d → d
A″	2.96	418.53		d → d

TDDFT calculated spectrum at somewhat shorter wavelength (244 nm). The CASPT2 and TDDFT calculated transitions >240 nm agree very well with each other. Both methods lead to the conclusion that the lowest energy experimental band at 546 nm originates from triplet d → d transitions.

Supplementary material

Crystallographic data have been deposited with the Cambridge Crystallographic Data Centre with deposition number CCDC 271563.

Acknowledgements

Crystallographic studies were financed by funds allocated by the Ministry of Scientific Research and Information Technology to the Institute of General and Ecological Chemistry, Technical University of Łódź. The GAUSSIAN GAUSSIAN03 calculations were carried out in the Wrocław Centre for Networking and Supercomputing, WCSS, Wrocław, Poland under Grant No. 51/96. Deepest thanks are due to Małgorzata Kałużyńska for her invaluable contribution to this work.

References

[1] (a) H. Le Bozec, D. Touchard, P.H. Dixneuf. *Adv. Organomet. Chem.*, **29**, 163 (1989); (b) R.M. Moriarty, U.S. Gill, Y.-Y. Ku. *J. Organomet. Chem.*, **350**, 157 (1988); (c) R. Noyori, S. Hashiguchi. *Acc. Chem. Res.*, **30**, 97 (1997); (d) M.A. Bennett, In *Comprehensive Organometallic Chemistry II*, E.W. Abel, F.G.A. Stone, G. Wilkinson (Eds), Vol. 7, Pergamon Press, Oxford (1995); (e) M.A. Bennett. *Coord. Chem. Rev.*, **166**, 225 (1997).

[2] G. Winkhaus, H. Singer. *J. Organomet. Chem.*, **7**, 487 (1967).

[3] (a) I. de los Rios, M.J. Tenerio, M.A.J. Tenorio, M.C. Puerta, P. Valerga. *J. Organomet. Chem.*, **525**, 57 (1996); (b) A. Schlüter, K. Bieber, W.S. Sheldrick. *Inorg. Chim. Acta*, **340**, 35 (2002); (c) Y. Chen, M. Valentini, P.S. Pregosin, A. Albinati. *Inorg. Chim. Acta*, **327**, 4 (2002); (d) A. Singh, N. Singh, D.S. Pandey. *J. Organomet. Chem.*, **642**, 48 (2002).

[4] (a) B. de Clercq, F. Verpoort. *J. Molec. Catal. A: Chem.*, **180**, 67 (2002); (b) A. Kathó, D. Carmona, F. Viguri, C.D. Remacha, J. Kovács, F. Joó, L.A. Oro. *J. Organomet. Chem.*, **593–594**, 299 (2000); (c) K. Mashima, K. Kusano, N. Sato, Y. Matsumura, K. Nozaki, H. Kumobayashi, N. Sayo, Y. Hori, T. Ishizaki, S. Akutagawa, H. Takaya. *J. Org. Chem.*, **59**, 3064 (1994); (d) S. Hashiguchi, A. Fujii, J. Takehara, T. Ikariya, R. Noyori. *J. Am. Chem. Soc.*, **117**, 7562 (1995); (e) A. Fujii, S. Hashiguchi, N. Uematsu, T. Ikariya, R. Noyori. *J. Am. Chem. Soc.*, **118**, 2521 (1996); (f) A.W. Stumpf, E. Saive, A. Demonceau, A.F. Noels. *J. Chem. Soc., Chem. Commun.*, **11**, 1127 (1995).

[5] (a) C.S. Allardyce, P.J. Dyson, D.J. Ellis, S.L. Heath. *J. Chem. Soc., Chem. Commun.*, **15**, 1396 (2001); (b) H. Chen, J.A. Parkinson, S. Parsons, R.A. Coxall, R.O. Gould, P.J. Sadler. *J. Am. Chem. Soc.*, **124**, 3064 (2002); (c) R.E. Aird, J. Cummings, A.A Ritchie, M. Muir, R.E. Morris, H. Chen, P.J. Sadler, D.I. Jodrell. *Brit. J. Cancer*, **86**, 1652 (2002); (d) R.E. Morris, R.E. Aird, P. Del, S. Murdoch, H. Chen, J. Cummings, N.D. Hughes, S. Parsons, A. Parkin, G. Boyd, D.I. Jodrell, P.J. Sadler. *J. Med. Chem.*, **44**, 3616 (2001).

[6] (a) P.H. Freeman, P.A. Worthington, W.G. Rathmell. *Eur. Pat. Appl.*, EP 0044 407 (1982); (b) J.L. Hilton. *J. Agric. Food Chem.*, **17**, 192 (1969); (c) C.K. Joshi, K. Dubey. *Phamazie*, **34**, 801 (1979).

[7] (a) H.O. Bayer, R.S. Cook, W.C. von Meyer. US Patent, **3**, 821 (1974); (b) J. Singh Idrissi, N.K. Singh. *Proc. Indian Acad. Sci.*, (*Chem. Sci.*), **93**, 125 (1984); (c) K.P. Parry, P.A. Worthington, W.G. Rathmell. *Eur. Pat. Appl.*, **15**, 756 (1980).

[8] (a) S. Trofimenko. *Chem. Rev.*, **93**, 943 (1993); (b) R. Mukherjee. *Coord. Chem. Rev.*, **203**, 151 (2000); (c) G. La Monica, G.A. Ardizzoia. *Prog. Inorg. Chem.*, **46**, 151 (1997); (d) A.P. Sadimenko, S.S. Basson. *Coord. Chem. Rev.*, **147**, 247 (1996); (e) A.A. Batista, I.S. Thorburn, B.R. James, S.J. Rettig, R.G. Ball. *Proc. 6th Int. Symp. Homogeneous Catalysis*, Vancouver, Canada (1988), P-123.

[9] (a) P.C. Hohenberg, W. Kohn, L.J. Sham. *Adv. Quantum Chem.*, **21**, 7 (1990); (b) W. Kohn, A.D. Becke, R.G. Parr. *J. Phys. Chem.*, **100**, 12974 (1996); (c) R.G. Parr, W. Yang. *Ann. Rev. Phys. Chem.*, **46**, 701 (1995); (d) E.J. Baerends, O.V. Gritsenko. *J. Phys. Chem. A*, **101**, 5383 (1997); (e) T. Ziegler. *Chem. Rev.*, **91**, 651 (1991).

[10] (a) M.E. Casida. In *Recent Advances in Density Functional Methods*, D.P. Chong (Ed.), Vol. 1, World Scientific, Singapore (1995); (b) M.E. Casida. In *Recent Developments and Applications of Modern Density Functional Theory*, *Theoretical and Computational Chemistry*, J.M. Seminario (Ed.), Vol. 4, p. 391, Elsevier, Amsterdam (1996); (c) M.E. Casida, C. Jamorski, K.C. Casida, D.R. Salahub. *J. Chem. Phys.*, **108**, 4439 (1998).
[11] (a) C. Adamo, V. Barone. *Theor. Chim. Acta*, **105**, 885 (2001); (b) S.J.A. van Gisbergen, J.A. Groeneveld, A. Rosa, J.G. Snijders, E.J. Baerends. *J. Phys. Chem. A*, **103**, 6835 (1999); (c) A. Rosa, E.J. Baerends, S.J.A. van Gisbergen, E. van Lenthe, J.A. Groeneveld, J.G. Snijders. *J. Am. Chem. Soc.*, **121**, 10356 (1999); (d) J.-F. Guillemoles, V. Barone, L. Joubert, C. Adamo. *J. Phys. Chem. A*, **106**, 11354 (2002); (e) J.E. Monat, J.H. Rodriguez, J.K. McCusker. *J. Phys. Chem. A*, **106**, 7399 (2002); (f) S. Fantacci, F. De Angelis, A. Selloni. *J. Am. Chem. Soc.*, **125**, 4381 (2003).
[12] (a) A. Dreuw, M. Head-Gordon. *J. Am. Chem. Soc.*, **126**, 4007 (2004); (b) A. Dreuw, J.L. Weisman, M. Head-Gordon. *J. Chem. Phys.*, **119**, 2943 (2003); (c) O. Gritsenko, E.J. Baerends. *J. Chem. Phys.*, **121**, 655 (2004); (d) S. Záliš, N. Ben Amor, C. Daniel. *Inorg. Chem.*, **43**, 7978 (2004).
[13] M.A. Bennett, T.-N. Huang, T.W. Matheson, A.K. Smith. *Inorg. Synth.*, **21**, 74 (1982).
[14] *Gaussian* 03, *Revision B.03*, Gaussian, Inc., Pittsburgh PA (2003).
[15] A.D. Becke. *J. Chem. Phys.*, **98**, 5648 (1993).
[16] C. Lee, W. Yang, R.G. Parr. *Phys. Rev. B*, **37**, 785 (1988).
[17] B. Mennucci, J. Tomasi. *J. Chem. Phys.*, **106**, 5151 (1997).
[18] K. Eichkorn, F. Weigend, O. Treutler, R. Ahlrichs. *Theor. Chim. Acta*, **97**, 119 (1997).
[19] K. Andersson, B.O Roos. In *Modern Electronic Structure Theory*, D.R. Yarkony (Ed.), pp. 55–109 World Scientific, Singapore (1995).
[20] G. Karlström, R. Lindh, P.-Å. Malmqvist, B.O. Roos, U. Ryde, V. Veryazov, P.-O. Widmark, M. Cossi, B. Schimmelpfennig, P. Neograd, L. Seijo. *Comput. Mater. Sci.*, **28,**, 222 (2003).
[21] P.O. Widmark, P.A. Malmqvist, B.O. Roos. *Theor. Chim. Acta*, **77**, 291 (1990).
[22] A.D. Becke. *J. Chem. Phys.*, **98**, 5648 (1993).
[23] G.M. Sheldrick. *Acta Cryst.*, **A46**, 467 (1990).
[24] G.M. Sheldrick. *SHELXL97. Program for the Solution and Refinement of Crystal Structures*, University of Göttingen, Germany (1997).
[25] G.M. Sheldrick. *SHELXTL* 4.1, Siemens Crystallographic Research Systems (1990).
[26] *International Tables for Crystallography*, Vol. I, pp. 182–189, D. Reidel Publishing Company, Dordrecht, Holland (1983).
[27] U. Beck, W. Hummel, H.B. Burgi, A. Ludi. *Organometallics*, **6**, 20 (1993).
[28] F.B. McCormick, D.D. Cox, W.B. Gleason. *Organometallics*, **12**, 610 (1993).
[29] I.D. Brown. *Acta Cryst.*, **B48**, 553 (1992).
[30] I.D. Brown. *Acta Cryst.*, **B53**, 381 (1997).
[31] M. O'Keeffe, N.E. Brese. *J. Am. Chem. Soc.*, **113**, 3226 (1991).
[32] J.G. Małecki, J.O. Dzięgielewski, M. Jaworska, R. Kruszynski, T.J. Bartczak. *Polyhedron*, **23**, 885 (2004).
[33] G.J. Palenik. *Inorg. Chem.*, **42**, 2725 (2003).
[34] G.R. Desiraju, T. Steiner. *The Weak Hydrogen Bond in Structural Chemistry and Biology*, Oxford University Press, Oxford (1999).
[35] G.A. Jeffrey, W. Saenger. *Hydrogen Bonding in Biological Structures*, Springer-Verlag, Berlin (1994).
[36] R. Taylor, O. Kennard. *J. Am. Chem. Soc.*, **104**, 5063 (1982).